INTERNATIONAL JOURNAL FOR NUMERICAL METHODS IN FLUIDS
Int. J. Numer. Meth. Fluids 2005; **47**:45–74
Published online 17 November 2004 in Wiley InterScience (www.interscience.wiley.com). DOI: 10.1002/fld.802

A posteriori pointwise error estimation for compressible fluid flows using adjoint parameters and Lagrange remainder

A. K. Alekseev[1] and I. M. Navon[2,*,†]

[1]*Department of Aerodynamics and Heat Transfer, RSC, ENERGIA, Korolev, Moscow Region 141070, Russian Federation*
[2]*Department of Mathematics and C.S.I.T., Florida State University, Tallahassee, FL 32306-4120, U.S.A.*

SUMMARY

The pointwise error of a finite-difference calculation of supersonic flow is discussed. The local truncation error is determined by a Taylor series with the remainder being in a Lagrange form. The contribution of the local truncation error to the total pointwise approximation error is estimated via adjoint parameters. It is demonstrated by numerical tests that the results of the numerical calculation of gasdynamics parameter at an observation point may be refined and an error bound may be estimated. The results of numerical tests for the case of parabolized Navier–Stokes are presented as an illustration of the proposed method.

KEY WORDS: adjoint problem; *a posteriori* error estimation; parabolized Navier–Stokes

1. INTRODUCTION

At present, the Richardson extrapolation [1–3] is the most popular method for estimation of discretization error in CFD. Unfortunately, a correct use of Richardson extrapolation requires a set of grids to prove monotonous convergence and to determine the real order of the convergence for the considered solution. This may turn out to be very expensive from the viewpoint of computer resources. The reason for this situation is the existence of many effects that may change the nominal order of the grid convergence. The simplest example is the convergence order reduction in presence of shocks. For schemes of third and fourth accuracy order, reduction of the convergence rate was demonstrated in Reference [4] for the compression wave. The works of Efraimsson and Kreiss [5], Engquist and Sjogreen [6] and Roy *et al.* [7] confirm this effect. Spatial non-uniformity of the grid may also reduce the convergence rate [8].

*Correspondence to: I. M. Navon, Dirac Sci Lib Bldg, Room 470, School of Computational Science, Florida State University, Tallahasse, FL 32306-4120, U.S.A.
†E-mail: navon@csit.fsu.edu

Contract/grant sponsor: NSF; contract/grant number: ATM-0201808

Received 14 April 2004
Revised 8 September 2004

An alternative approach for *a posteriori* error estimation has intensively been developed for the last decade (References [9–35]). It is used for the estimation of error of some quantities of interest (goal functionals, point-wise parameters, etc.) using residual (truncation error) and adjoint (dual) equations. In Reference [28] this approach is used for wave equations, in Reference [31] it is used for transport equation. In References [13–15] *a posteriori* error estimation is obtained for Navier–Stokes and Euler equations. In these works the Galerkin method is used for the local error estimation while the adjoint equations are used for calculating their weights in the target functional error. A similar approach was used in References [16–27] for the refinement of practically useful functionals both by finite-element and finite-difference methods. The local truncation error (residual) was estimated through the action of differential operator on interpolated solution, while its contribution to the functional was calculated using an adjoint problem. The error is demonstrated to be composed of two components, the first being computable using adjoint parameters and residual while the second being incomputable (depending on errors of solution of both primal and adjoint problems). In References [16–18] the information on the spatial distribution of the residuals was used for mesh refining (for diminishing the incomputable error) above the estimation of the computable error. A survey of *a posteriori* error estimation using the adjoint equations may be found in Reference [24].

In the present work we consider another approach for the estimation of the computable error if compared with References [16–27]. It is based on a differential approximation (DA) [36] instead of on residual estimation and is more natural for finite-differences. This provides certain peculiarities both in applicability domain and the features of the methods. We use a local truncation error determined by a Taylor series with the remainder in Lagrange form and adjoint equations in a continuous form. This enables us to correct the error and to obtain an asymptotic error bound for refined solution. The refinement and the error bound are obtained on the same grid as that employed for the primal problem solution and require identical computer time. This approach was used for heat transfer equation in References [37, 38]. Herein, we consider an application of the approach to a finite-difference approximation of the parabolized Navier–Stokes (PNS) and Euler equations.

For illustrating the main idea we use the equation $(\partial\tilde{\rho}/\partial t)+(\partial\tilde{\rho}/\partial x)=0$ and its finite-difference approximation

$$\frac{\rho_k^{n+1}-\rho_k^n}{\tau}+\frac{\rho_{k+1}^n-\rho_k^n}{h_k}=0$$

let the solution be smooth enough to possess all necessary derivatives to be bounded. Let us use the Taylor series with the remainder in Lagrange form (parameters $\alpha_k^n\in(0,1),\beta_k^n\in(0,1)$, are unknown).

$$\frac{\partial\rho}{\partial t}+\frac{\partial\rho}{\partial x}+\frac{1}{2}\left(\tau\frac{\partial^2\rho(t_n+\beta_k^n\tau,x_k)}{\partial t^2}+h_k\frac{\partial^2\rho(t_n,x_k+\alpha_k^n h_k)}{\partial x^2}\right)=0 \tag{1}$$

Thus, a finite-difference equation is equivalent to an approximated equation with an additional perturbation term. Mathematical details of this equivalence may be found in References [1, 36].

Let us find the error of the functional $\varepsilon = \int_\Omega \rho(t,x)\delta(x - x_{\text{est}})\delta(t - t_{\text{est}})\,\mathrm{d}t\,\mathrm{d}x$ as a function of truncation error. For this purpose let us introduce the Lagrangian

$$L = \varepsilon + \int_\Omega \left(\frac{\partial \rho}{\partial t} + \frac{\partial \rho}{\partial x} \right) \psi \,\mathrm{d}t\,\mathrm{d}x$$

It may be shown from this Lagrangian variation that for solutions of

$$\textit{direct}\ \frac{\partial \rho}{\partial t} + \frac{\partial \rho}{\partial x} = 0 \ \text{ and } \ \textit{adjoint}\ \frac{\partial \psi}{\partial t} + \frac{\partial \psi}{\partial x} - \delta(x - x_{\text{est}})\delta(t - t_{\text{est}}) = 0 \ \textit{problems} \tag{2}$$

the variation of the functional caused by the truncation error component (from x derivative) equals

$$\Delta\varepsilon(\delta\rho_x) = \int_\Omega \left(h_k \frac{\partial^2 \rho(t_n, x_k + \alpha_k^n h_k)}{\partial x^2} \right) \psi \,\mathrm{d}x\,\mathrm{d}t \tag{3}$$

Its discrete form may be recast to assume the form

$$\Delta\varepsilon(\delta\rho_x) = \frac{1}{2} \sum_{k=1,n=1}^{Nx,Nt} \left(h_k \frac{\partial^2 \rho(t_n, x_k + \alpha_k^n h_k)}{\partial x^2} \right) \psi_k^n h_k \tau \tag{4}$$

Using a Taylor expansion, expression (4) may be written as

$$\Delta\varepsilon(\delta\rho_x) = \frac{1}{2} \sum_{k=1,n=1}^{Nx,Nt} \left(h_k \frac{\partial^2 \rho(t_n, x_k)}{\partial x^2} + \alpha_k^n h_k^2 \frac{\partial^3 \rho(t_n, x_k)}{\partial x^3} \right) \psi_k^n h_k \tau \tag{5}$$

The first part of sum (5) may be used for refining the functional; the error is caused by the second part due to unknown parameters α_k^n. These parameters belong to the unit interval $\alpha_k^n \in (0,1)$, so we may obtain a bound of this expression

$$\frac{1}{2} \sum_{k=1,n=1}^{Nx,Nt} \alpha_k^n h_k^3 \frac{\partial^3 \rho(t_n, x_k)}{\partial x^3} \psi_k^n \tau \leqslant \frac{1}{2} \sum_{k=1,n=1}^{Nx,Nt} \left| \tau h_k^3 \frac{\partial^3 \rho(t_n, x_k)}{\partial x^3} \psi_k^n \right| = \Delta\rho_x^{\text{sup}} \tag{6}$$

Using such estimates for both co-ordinates we can determine a bound of the functional error after refinement

$$|\rho - \Delta\rho_t^{\text{corr}} - \Delta\rho_x^{\text{corr}} - \rho_{\text{exact}}| < \Delta\rho_x^{\text{sup}} + \Delta\rho_t^{\text{sup}} \tag{7}$$

This approach also provides an estimate of higher-order terms in (4). For example, an estimate of the second order over $\alpha_k^n h_k$ has the form

$$\sum_{k=1,n=2}^{Nx,Nt} \left(\frac{(\alpha_k^n h_k)^2}{2} h_k \frac{\partial^4 \rho(t_n, x_k)}{\partial x^4} \right) \psi_k^n h_k \tau < \sum_{k=1,n=2}^{Nx,Nt} \left| \frac{1}{2} h_k^4 \tau \psi_k^n \frac{\partial^4 \rho(t_n, x_k)}{\partial x^4} \right| = \Delta\rho_{x,2}^{\text{sup}} \tag{8}$$

For a second-order estimate we obtain

$$|\rho - \Delta\rho^{\text{corr}} - \rho_{\text{exact}}| < \Delta\rho_1^{\text{sup}} + \Delta\rho_2^{\text{sup}} \tag{9}$$

For an infinitely smooth solution we may write

$$|\rho - \Delta\rho_t^{\text{corr}} - \Delta\rho_x^{\text{corr}} - \rho_{\text{exact}}| < \sum_{s=1}^{\infty} \Delta\rho_{t,s}^{\text{sup}} + \sum_{s=1}^{\infty} \Delta\rho_{x,s}^{\text{sup}}$$

If all derivatives are bounded, these series converge due to

$$\sum_{k=1,n=2}^{Nx,Nt} \left| \frac{(\alpha_k^n h)^s}{s!} \frac{\partial^{s+2}\rho(t_n,x_k)}{\partial x^{s+2}} \psi_k^n h^2 \tau \right| < \mathrm{Ch}\frac{h^s}{s!}$$

Nevertheless, this does not guarantee the estimation to be small enough to be of a practical significance.

We should use numerical expressions for high-order derivatives in the above formulations. If the numerical solution has oscillations, these estimates may be too large and be of no practical use. So, the considered approach may be used only for finite difference schemes which are monotonous enough.

Expression (7) is correct for exact values of adjoint parameter. In reality, the adjoint problem is solved by some finite-difference method, so it contains some approximation error $\psi(t,x) = \psi_{\text{exact}}(t,x) + \Delta\psi(t,x)$. Hence, the estimation of the functional variation has a component determined by the adjoint problem error.

$$\Delta\varepsilon = \iint_\Omega \delta\rho\Delta\psi(t,x)\,\mathrm{d}t\,\mathrm{d}x \tag{10}$$

This term corresponds to the remaining error according to Reference [19] and is associated to the errors of approximation of both adjoint and primal equations. Works [16–18] concern a construction of a mesh for the minimization of this term. As an alternative, we may use the second-order adjoint equations [38–40] for calculating this term. If the primal and adjoint problems are solved by methods of order $O(h^p)$ and $O(h^a)$, this term is of $O(h^{p+a})$ order. For schemes of high enough order ($p \geqslant 2$ or $a \geqslant 2$) this term is asymptotically small if compared with error bounds determined by (6).

2. THE ESTIMATE OF APPROXIMATION ERROR FOR FINITE-DIFFERENCE CALCULATION OF A FLOW PARAMETER

Consider the discussed method of approximation error for estimating two-dimensional supersonic viscous flow, Figure 1.

The non-divergent form of PNS is used. The flow is calculated by march along the X-axis.

$$\frac{\partial(\rho U)}{\partial X} + \frac{\partial(\rho V)}{\partial Y} = 0 \tag{11}$$

$$U\frac{\partial U}{\partial X} + V\frac{\partial U}{\partial Y} + \frac{1}{\rho}\frac{\partial P}{\partial X} - \frac{1}{Re\,\rho}\frac{\partial^2 U}{\partial Y^2} = 0 \tag{12}$$

$$U\frac{\partial V}{\partial X} + V\frac{\partial V}{\partial Y} + \frac{1}{\rho}\frac{\partial P}{\partial Y} - \frac{4}{3\rho\,Re}\frac{\partial^2 V}{\partial Y^2} = 0 \tag{13}$$

$$U\frac{\partial e}{\partial X} + V\frac{\partial e}{\partial Y} + (\kappa-1)e\left(\frac{\partial U}{\partial X} + \frac{\partial V}{\partial Y}\right) - \frac{1}{\rho}\frac{\gamma}{Re\,Pr}\frac{\partial^2 e}{\partial Y^2} - \frac{1}{\rho}\frac{4}{3Re}\left(\frac{\partial U}{\partial Y}\right)^2 = 0 \tag{14}$$

$$P = \rho RT, \quad e = C_v T = \frac{RT}{\gamma - 1}, \quad (X,Y) \in \Omega = (0 < X < X_{\max},\ 0 < Y < Y_{\max})$$

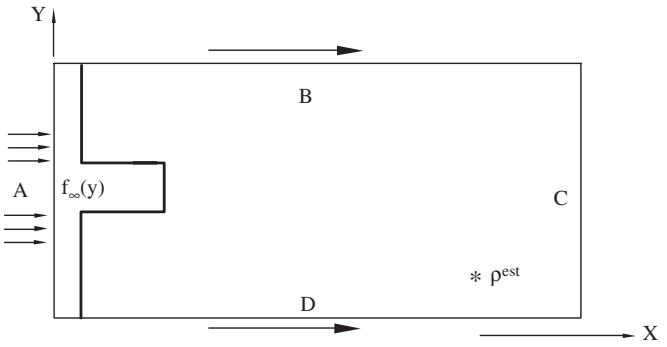

Figure 1. Flow sketch. A—entrance boundary, B, D—lateral boundaries, *—location of estimated parameter.

On inflow boundary (A $(X=0)$, Figure 1) we have $e(0,Y)=e_\infty(Y)$, $\rho(0,Y)=\rho_\infty(Y)$), $U(0,Y)=U_\infty(Y)$, $V(0,Y)=V_\infty(Y)$; On lateral boundaries B, D $(Y=0,\ Y=Y_{\max})$ the conditions $\partial f/\partial Y=0$ $(f^i=(\rho,U,V,e))$ are imposed.

The density at some point is considered as an estimated parameter. Let us write the estimated value $\rho(X^{\text{est}},Y^{\text{est}})$ in the form of a functional.

$$\rho^{\text{est}}=\varepsilon=\int_\Omega \rho(X,Y)\delta(Y-Y^{\text{est}})\delta(X-X^{\text{est}})\,\mathrm{d}X\,\mathrm{d}Y \tag{15}$$

We need to calculate the gradient of target functional with respect to local disturbances (truncation error) δf^i. It is known that the most efficient way for the gradient calculation is based on using the adjoint equations [41]. These equations may be obtained in a standard way by unifying in a single Lagrangian the estimated functional and the weak formulation of the flow dynamics problem. Herein, we present the result. Additional details may be found in References [42, 43].

3. ADJOINT PROBLEM

$$\begin{aligned}
&U\frac{\partial\Psi_\rho}{\partial X}+V\frac{\partial\Psi_\rho}{\partial Y}+(\gamma-1)\frac{\partial(\Psi_V e/\rho)}{\partial Y}+(\gamma-1)\frac{\partial(\Psi_U e/\rho)}{\partial X}\\
&-\frac{\gamma-1}{\rho}\left(\frac{\partial e}{\partial Y}\Psi_V+\frac{\partial e}{\partial X}\Psi_U\right)+\left(\frac{1}{\rho^2}\frac{\partial P}{\partial X}-\frac{1}{\rho^2 Re}\frac{\partial^2 U}{\partial Y^2}\right)\Psi_U\\
&+\frac{1}{\rho^2}\left(\frac{\partial P}{\partial Y}-\frac{4}{3Re}\frac{\partial^2 V}{\partial Y^2}\right)\Psi_V-\frac{1}{\rho^2}\left(\frac{\gamma}{Re\,Pr}\frac{\partial^2 e}{\partial Y^2}+\frac{4}{3Re}\left(\frac{\partial U}{\partial Y}\right)^2\right)\Psi_e\\
&-\delta(X-X^{\text{est}})\delta(Y-Y^{\text{est}})=0
\end{aligned} \tag{16}$$

The source in (16) corresponds to the location of the estimated parameter.

$$U\frac{\partial\Psi_U}{\partial X}+\frac{\partial(\Psi_U V)}{\partial Y}+\rho\frac{\partial\Psi_\rho}{\partial X}-\left(\frac{\partial V}{\partial X}\Psi_V+\frac{\partial e}{\partial X}\Psi_e\right)+\frac{\partial}{\partial X}\left(\frac{P}{\rho}\Psi_e\right)$$
$$+\frac{\partial^2}{\partial Y^2}\left(\frac{1}{\rho\,Re}\Psi_U\right)-\frac{\partial}{\partial Y}\left(\frac{8}{3Re}\frac{\partial U}{\partial Y}\Psi_e\right)=0 \tag{17}$$

$$\frac{\partial(U\Psi_V)}{\partial X}+V\frac{\partial\Psi_V}{\partial Y}-\left(\frac{\partial U}{\partial Y}\Psi_U+\frac{\partial e}{\partial Y}\Psi_e\right)$$
$$+\rho\frac{\partial\Psi_\rho}{\partial Y}+\frac{\partial}{\partial Y}\left(\frac{P}{\rho}\Psi_e\right)+\frac{4}{3Re}\frac{\partial^2}{\partial Y^2}\left(\frac{\Psi_V}{\rho}\right)=0 \tag{18}$$

$$\frac{\partial(U\Psi_e)}{\partial X}+\frac{\partial(V\Psi_e)}{\partial Y}-\frac{\gamma-1}{\rho}\left(\frac{\partial\rho}{\partial Y}\Psi_V+\frac{\partial\rho}{\partial X}\Psi_U\right)-(\gamma-1)\left(\frac{\partial U}{\partial X}+\frac{\partial V}{\partial Y}\right)\Psi_e$$
$$+(\gamma-1)\frac{\partial\Psi_V}{\partial Y}+(\gamma-1)\frac{\partial\Psi_U}{\partial X}+\frac{\gamma}{Re\,Pr}\frac{\partial^2}{\partial Y^2}\left(\frac{\Psi_e}{\rho}\right) \tag{19}$$

Parameters $(\Psi_\rho,\Psi_U,\Psi_V,\Psi_e)$ are the adjoint analogs of density, velocity components, and energy.

$$\textit{Initial conditions } C\ (X=X_{\max})\text{: } \Psi_{\rho,U,V,e}|^{X=X_{\max}}=0 \tag{20}$$

Expression for Ψ_ρ corresponds to the location of an estimated parameter on the boundary $X_{\max}$.

$$\textit{Boundary conditions on } B,D\ (Y=0;\ Y=Y_{\max})\text{: } \frac{\partial\Psi_f}{\partial Y}=0 \tag{21}$$

Adjoint problem is calculated in the reverse direction along X. For point-wise error estimation the equations have singular sources (Dirac's delta functions, Equation (16)). Unfortunately, the regularity both of parabolized Navier–Stokes and corresponding adjoint system are unknown. Both these systems of equations are of mixed hyperbolic–parabolic nature. According to Reference [44] the heat transfer (parabolic) problem with similar source is well-posed for $\Psi(t,x)\in H^{-\alpha}(\Omega)$, $\alpha/n>\frac{1}{2}$, $\Omega\in R^n$. From this analogy, the considered problem may be well-posed in $H^{-1}(\Omega)$ a fact that engenders corresponding computational difficulties. However, if we smooth the source term according to References [45, 46], we may obtain a solution $\Psi_s(t,x)\in H^\beta(\Omega)$, $\beta>1$ (although containing an error proportional to smoothing parameter $s, s>0$, which may be as small as necessary). Methods of finite difference solution for such equations are also presented in References [45, 46].

The target functional variation as a function of the truncation error has the following form:

$$\delta\varepsilon=\iint_\Omega(\delta\rho\Psi_\rho+\delta U\Psi_U+\delta V\Psi_V+\delta e\Psi_e)\,\mathrm{d}X\,\mathrm{d}Y \tag{22}$$

In tests presented below we compare the results of finite-difference calculations with the analytical solutions corresponding to inviscid gas flows. In this context, the influence of viscous terms in Equations (11)–(14) on an estimated parameter is of interest. We consider the solution of equations without viscosity as a non-perturbed one. Let the viscous terms disturb this solution. For example, for the longitudinal velocity undisturbed values are governed by the equation

$$U\frac{\partial U}{\partial X}+V\frac{\partial U}{\partial Y}=0$$

while the disturbed ones are governed by

$$U\frac{\partial \tilde{U}}{\partial X}+V\frac{\partial \tilde{U}}{\partial Y}-\frac{1}{Re\,\rho}\frac{\partial^2 \tilde{U}}{\partial Y^2}=0$$

Then the variation of the target functional due to viscous terms assumes the form

$$\delta\varepsilon=-\int_\Omega\left(\frac{1}{Re\,\rho}\frac{\partial^2 \tilde{U}}{\partial Y^2}\Psi_U+\cdots\right)\mathrm{d}\Omega \tag{23}$$

In contrast to (16)–(19), the corresponding adjoint equations have no viscous terms.

Certainly, this approach is valid only when influence of viscous terms is small enough, i.e. when they do not cause a radical change of flow structure.

Another reason for the development of this technique arises for discontinuities that are typical of supersonic flows described by Euler equations, for example. The approach based on differential approximation is not applicable for supersonic Euler equations due to unbound derivatives. Nevertheless, we may use parabolized Navier–Stokes for basic flow calculation, consider viscous terms as a perturbation, and calculate the effect of this perturbation on the solution. This may enable us to expand the applicability of the differential approximation approach to discontinuous flows described by Euler equations.

4. FINITE DIFFERENCE SCHEME

To study the approximation error herein we need a finite difference scheme having largest truncation error. As a consequence, we use a first-order scheme, the convective terms being obtained by upwind differences [47]. Nevertheless, several terms are approximated by symmetrical differences with the result that they have second order. A finite-difference scheme (for $V_k^n>0$ option) is presented below. It contains two steps, predictor and corrector. Both steps are calculated implicitly, using the three point Thomas algorithm. The tilde marks parameters computed at the first step.

Predictor:

$$U_k^n\frac{\tilde{\rho}_k^{n+1}-\rho_k^n}{h_x}+\rho_k^n\frac{U_k^n-U_k^{n-1}}{h_x}+V_k^n\frac{\tilde{\rho}_k^{n+1}-\tilde{\rho}_{k-1}^{n+1}}{h_y}+\rho_k^n\frac{V_{k+1}^n-V_{k-1}^n}{2h_y}=0 \tag{24}$$

$$U_k^n\frac{\tilde{U}_k^{n+1}-U_k^n}{h_x}+V_k^n\frac{\tilde{U}_k^{n+1}-\tilde{U}_{k-1}^{n+1}}{h_y}+\frac{P_k^n-P_k^{n-1}}{h_x\rho_k^n}-\frac{1}{Re\,\rho_k^n}\frac{\tilde{U}_{k+1}^{n+1}-2\tilde{U}_k^{n+1}-\tilde{U}_{k-1}^{n+1}}{h_y^2}=0 \tag{25}$$

$$U_k^n \frac{\tilde{V}_k^{n+1} - V_k^n}{h_x} + V_k^n \frac{\tilde{V}_k^{n+1} - \tilde{V}_{k-1}^{n+1}}{h_y} + \frac{P_{k+1}^n - P_{k-1}^n}{2h_y \rho_k^n} - \frac{4}{3Re\,\rho_k^n} \frac{\tilde{V}_{k+1}^{n+1} - 2\tilde{V}_k^{n+1} - \tilde{V}_{k-1}^{n+1}}{h_y^2} = 0 \tag{26}$$

$$U_k^n \frac{\tilde{e}_k^{n+1} - e_k^n}{h_x} + V_k^n \frac{\tilde{e}_k^{n+1} - \tilde{e}_{k-1}^{n+1}}{h_y} + (\gamma - 1) e_k^n \frac{U_k^n - U_k^{n-1}}{h_x} + (\gamma - 1) e_k^n \frac{V_{k+1}^n - V_{k-1}^n}{2h_y}$$
$$- \frac{\gamma}{Re\,Pr\,\rho_k^n} \frac{\tilde{e}_{k+1}^{n+1} - \tilde{2}e_k^{n+1} - \tilde{e}_{k-1}^{n+1}}{h_y^2} + \Phi = 0 \tag{27}$$

Corrector:

$$\tilde{U}_k^{n+1} \frac{\rho_k^{n+1} - \rho_k^n}{h_x} + \tilde{\rho}_k^{n+1} \frac{\tilde{U}_k^{n+1} - U_k^n}{h_x} + \tilde{V}_k^{n+1} \frac{\rho_k^{n+1} - \rho_{k-1}^{n+1}}{h_y} + \tilde{\rho}_k^{n+1} \frac{\tilde{V}_{k+1}^{n+1} - \tilde{V}_{k-1}^{n+1}}{2h_y} = 0 \tag{28}$$

$$\tilde{U}_k^{n+1} \frac{U_k^{n+1} - U_k^n}{h_x} + \tilde{V}_k^{n+1} \frac{U_k^{n+1} - U_{k-1}^{n+1}}{h_y} + \frac{\tilde{P}_k^{n+1} - P_k^n}{h_x \tilde{\rho}_k^{n+1}}$$
$$- \frac{1}{Re\,\tilde{\rho}_k^{n+1}} \frac{U_{k+1}^{n+1} - 2U_k^{n+1} - U_{k-1}^{n+1}}{h_y^2} = 0 \tag{29}$$

$$\tilde{U}_k^{n+1} \frac{V_k^{n+1} - V_k^n}{h_x} + \tilde{V}_k^{n+1} \frac{V_k^{n+1} - V_{k-1}^{n+1}}{h_y} + \frac{\tilde{P}_{k+1}^{n+1} - \tilde{P}_{k-1}^{n+1}}{2h_y \rho_k^n}$$
$$- \frac{4}{3Re\,\rho_k^n} \frac{V_{k+1}^{n+1} - 2V_k^{n+1} - V_{k-1}^{n+1}}{h_y^2} = 0 \tag{30}$$

$$\tilde{U}_k^{n+1} \frac{e_k^{n+1} - e_k^n}{h_x} + \tilde{V}_k^{n+1} \frac{e_k^{n+1} - e_{k-1}^{n+1}}{h_y} + (\gamma - 1) \tilde{e}_k^{n+1} \frac{\tilde{U}_k^{n+1} - U_k^n}{h_x} + (\gamma - 1) e_k^n \frac{\tilde{V}_{k+1}^{n+1} - \tilde{V}_{k-1}^{n+1}}{2h_y}$$
$$- \frac{\gamma}{Re\,Pr\,\tilde{\rho}_k^{n+1}} \frac{e_{k+1}^{n+1} - 2e_k^{n+1} - e_{k-1}^{n+1}}{h_y^2} + \Phi = 0 \tag{31}$$

The finite difference scheme has a similar form for the adjoint system. The main feature is the presence of the source term $\delta(X - X^{\text{est}})\delta(Y - Y^{\text{est}})$ in (16), which is related to the location of estimated point. For fine enough grids a mollification (smooth approximation of δ-function) may be necessary for approximation of this source term [10]. The methods of finite difference solution of equations with such sources are presented in References [45, 46].

5. ESTIMATION OF THE TRUNCATION ERROR

The total approximation error depends on a local truncation error. In order to determine it, we expand finite differences in Taylor series with Lagrange remainder. For illustration let us present this estimation for one of finite-difference terms in (29).

$$U_k^n \frac{U_k^n - U_k^{n-1}}{h_x} = U \frac{\partial U}{\partial X} - \frac{1}{2} U_k^n \left(h_{x,n} \frac{\partial^2 U(X_n - \alpha_k^n h_{x,n}, Y_k)}{\partial X^2} \right) \tag{32}$$

The corresponding component of target functional variation $\Delta\rho_{\text{est}}$ assumes the form

$$\Delta\varepsilon(\delta U) = -\frac{1}{2} \int_\Omega \left(h_{x,n} \frac{\partial^2 U(X_n - \alpha_k^n h_{x,n}, Y_k)}{\partial X^2} \right) U \Psi_U \, \mathrm{d}X \, \mathrm{d}Y \tag{33}$$

Its discrete form is

$$\Delta\varepsilon(\delta U) = -\frac{1}{2} \sum_{k=1,n=2}^{N,Nx} \left(h_x \frac{\partial^2 U(X_n - \alpha_k^n h_x, Y_k)}{\partial X^2} \right) U_k^n \Psi_{U,k}^n h_{y,k} h_{x,n}$$

For a first-order over $\alpha_k^n h_{x,n}$ it may be presented as

$$\Delta\varepsilon(\delta U) = -\frac{1}{2} \sum_{k=1,n=2}^{N,Nx} \left(h_{x,n} \frac{\partial^2 U(X_n, Y_k)}{\partial X^2} - \alpha_k^n h_{x,n}^2 \frac{\partial^3 U(X_n, Y_k)}{\partial X^3} \right) U_k^n \Psi_{U,k}^n h_{y,k} h_{x,n} \tag{34}$$

The first part of this sum may be used for refining of the functional

$$\Delta\rho_x^{\text{corr}} = -\frac{1}{2} \sum_{k=1,n=2}^{N,Nx} \frac{\partial^2 U(X_n, Y_k)}{\partial X^2} U_k^n \Psi_{U,k}^n h_{y,k} h_{x,n}^2 \tag{35}$$

Non-eliminated error is engendered by the second part of (34). It has an upper bound

$$\frac{1}{2} \sum_{k=1,n=2}^{N,Nx} \alpha_k^n h_{x,n}^3 \frac{\partial^3 U(X_n, Y_k)}{\partial X^3} U_k^n \Psi_{U,k}^n h_{y,k} \leqslant \frac{1}{2} \sum_{k=1,n=2}^{N,Nx} \left| h_{y,k} h_{x,n}^3 \frac{\partial^3 U(X_n, Y_k)}{\partial X^3} U_k^n \Psi_{U,k}^n \right| = \Delta\rho_x^{\text{sup}} \tag{36}$$

Total refinement of the functional determined by all first-order terms of finite-difference scheme (28)–(31) is as follows:

$$\begin{aligned}
\Delta\rho^{\text{corr}} = & -\frac{1}{2} \sum_{k=1,n=2}^{N,Nx} \frac{\partial^2 \rho(X_n, Y_k)}{\partial X^2} U_k^n \Psi_{\rho,k}^n h_{y,k} h_{x,n}^2 - \frac{1}{2} \sum_{k=1,n=2}^{N,Nx} \frac{\partial^2 \rho(X_n, Y_k)}{\partial Y^2} |V_k^n| \Psi_{\rho,k}^n h_{x,k} h_{y,n}^2 \\
& -\frac{1}{2} \sum_{k=1,n=2}^{N,Nx} \frac{\partial^2 U(X_n, Y_k)}{\partial X^2} \rho_k^n \Psi_{\rho,k}^n h_{y,k} h_{x,n}^2 \\
& -\frac{1}{2} \sum_{k=1,n=2}^{N,Nx} \frac{\partial^2 U(X_n, Y_k)}{\partial X^2} U_k^n \Psi_{U,k}^n h_{y,k} h_{x,n}^2 - \frac{1}{2} \sum_{k=1,n=2}^{N,Nx} \frac{\partial^2 U(X_n, Y_k)}{\partial Y^2} |V_k^n| \Psi_{U,k}^n h_{x,k} h_{y,n}^2
\end{aligned}$$

$$-\frac{\gamma-1}{2\rho_k^n}\sum_{k=1,n=2}^{N,Nx}\frac{\partial^2\rho(X_n,Y_k)}{\partial X^2}e_k^n\Psi_{U,k}^n h_{y,k}h_{x,n}^2-\frac{\gamma-1}{2}\sum_{k=1,n=2}^{N,Nx}\frac{\partial^2 e(X_n,Y_k)}{\partial X^2}\Psi_{U,k}^n h_{y,k}h_{x,n}^2$$

$$-\frac{1}{2}\sum_{k=1,n=2}^{N,Nx}\frac{\partial^2 V(X_n,Y_k)}{\partial X^2}U_k^n\Psi_{V,k}^n h_{y,k}h_{x,n}^2-\frac{1}{2}\sum_{k=1,n=2}^{N,Nx}\frac{\partial^2 V(X_n,Y_k)}{\partial Y^2}|V_k^n|\Psi_{V,k}^n h_{x,k}h_{y,n}^2$$

$$-\frac{1}{2}\sum_{k=1,n=2}^{N,Nx}\frac{\partial^2 e(X_n,Y_k)}{\partial X^2}U_k^n\Psi_{e,k}^n h_{y,k}h_{x,n}^2-\frac{1}{2}\sum_{k=1,n=2}^{N,Nx}\frac{\partial^2 e(X_n,Y_k)}{\partial Y^2}|V_k^n|\Psi_{e,k}^n h_{x,k}h_{y,n}^2$$

$$-\frac{\gamma-1}{2}\sum_{k=1,n=2}^{N,Nx}\frac{\partial^2 U(X_n,Y_k)}{\partial X^2}e_k^n\Psi_{e,k}^n h_{y,k}h_{x,n}^2 \tag{37}$$

Total expression for error bound caused by the first-order terms of (28)–(31) has the form

$$\Delta\rho^{\sup}=\frac{1}{2}\sum_{k=1,n=2}^{N,Nx}\left|\frac{\partial^3\rho(X_n,Y_k)}{\partial X^3}U_k^n\Psi_{\rho,k}^n\right|h_{y,k}h_{x,n}^3+\frac{1}{2}\sum_{k=1,n=2}^{N,Nx}\left|\frac{\partial^3\rho(X_n,Y_k)}{\partial Y^3}V_k^n\Psi_{\rho,k}^n h_{x,k}h_{y,n}^3\right|$$

$$+\frac{1}{2}\sum_{k=1,n=2}^{N,Nx}\left|\frac{\partial^3 U(X_n,Y_k)}{\partial X^3}\rho_k^n\Psi_{\rho,k}^n\right|h_{y,k}h_{x,n}^3$$

$$+\frac{1}{2}\sum_{k=1,n=2}^{N,Nx}\left|\frac{\partial^3 U(X_n,Y_k)}{\partial X^3}U_k^n\Psi_{U,k}^n\right|h_{y,k}h_{x,n}^3+\frac{1}{2}\sum_{k=1,n=2}^{N,Nx}\left|\frac{\partial^3 U(X_n,Y_k)}{\partial Y^3}V_k^n\Psi_{U,k}^n\right|h_{x,k}h_{y,n}^3$$

$$+\frac{\gamma-1}{2\rho_k^n}\sum_{k=1,n=2}^{N,Nx}\left|\frac{\partial^3\rho(X_n,Y_k)}{\partial X^3}e_k^n\Psi_{U,k}^n\right|h_{y,k}h_{x,n}^3+\frac{\gamma-1}{2}\sum_{k=1,n=2}^{N,Nx}\left|\frac{\partial^3 e(X_n,Y_k)}{\partial X^3}\Psi_{U,k}^n\right|h_{y,k}h_{x,n}^3$$

$$+\frac{1}{2}\sum_{k=1,n=2}^{N,Nx}\left|\frac{\partial^3 V(X_n,Y_k)}{\partial X^3}U_k^n\Psi_{V,k}^n h_{y,k}h_{x,n}^3\right|+\frac{1}{2}\sum_{k=1,n=2}^{N,Nx}\left|\frac{\partial^3 V(X_n,Y_k)}{\partial Y^3}V_k^n\Psi_{V,k}^n\right|h_{x,k}h_{y,n}^3$$

$$+\frac{1}{2}\sum_{k=1,n=2}^{N,Nx}\left|\frac{\partial^3 e(X_n,Y_k)}{\partial X^3}U_k^n\Psi_{e,k}^n\right|h_{y,k}h_{x,n}^3+\frac{1}{2}\sum_{k=1,n=2}^{N,Nx}\left|\frac{\partial^3 e(X_n,Y_k)}{\partial Y^3}V_k^n\Psi_{e,k}^n\right|h_{x,k}h_{y,n}^2$$

$$+\frac{\gamma-1}{2}\sum_{k=1,n=2}^{N,Nx}\left|\frac{\partial^3 U(X_n,Y_k)}{\partial X^3}e_k^n\Psi_{e,k}^n\right|h_{y,k}h_{x,n}^3 \tag{38}$$

Similar expressions are obtained for the convective terms of second-order accuracy and for the viscous terms. A bound of the refined functional error may be determined by these expressions as

$$|\rho-\Delta\rho^{\text{corr}}-\rho_{\text{exact}}|<\Delta\rho^{\sup} \tag{39}$$

This bound does not account for the incomputable error (expressions similar to (10)), or errors caused by boundary condition approximation, etc. It also uses derivatives0 whose boundedness cannot be proven at present. So, it requires a confirmation via numerical tests.

6. NUMERICAL TESTS

6.1. Continuous flow field

A comparison between computations by finite-differences and analytic expressions, and an analysis of error estimates is performed for Prandtl–Mayer flow. The error of flow density past the expansion fan was addressed (freestream Mach number $M = 4$, angle of flow rotation $\alpha = 10^\circ$).

Let us determine the approximation error using adjoint approach and compare it with the deviation of the finite-difference solution from analytic one. Figure 2 illustrates the density isolines in flowfield, Figure 3 illustrates the adjoint density isolines (a concentration of isolines

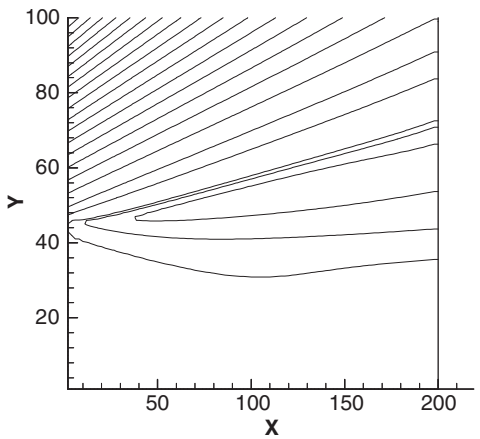

Figure 2. Isolines of density (Prandtl–Mayer flow).

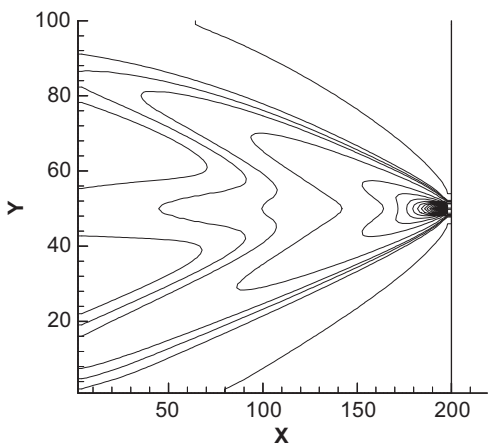

Figure 3. Isolines of adjoint density (concentration correlates with estimated point).

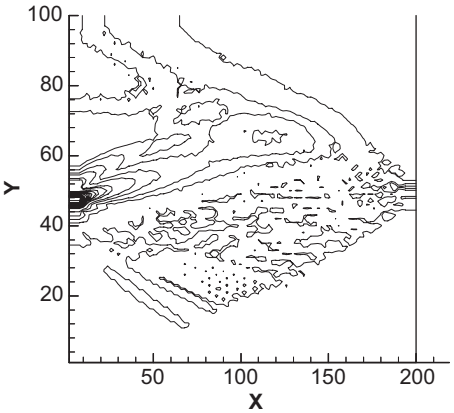

Figure 4. Isolines of density of error bound (38).

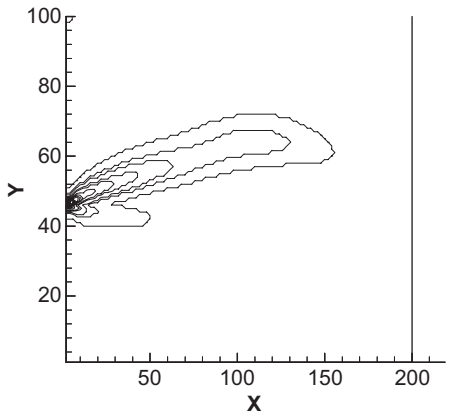

Figure 5. Isolines of error density caused by viscosity (23).

corresponds to a point of estimation). Figure 4 presents the spatial distribution of density of error bound (38), and Figure 5 depicts isolines of density of error caused by the viscous terms (23). Figures 4 and 5 determine those spatial regions that generate the main part of error for parameter at the estimated point. Results presented in Figures 2–5 correspond to calculations taking into account the viscosity (PNS, $Re = 1000$).

Figure 6 presents the relative error of flow density calculation for $Re = 1000$ as a function of the reciprocal of spatial step in Y direction (number of nodes). The part of error caused by viscous terms (21), relative deviation $(\rho - \Delta\rho^{\mathrm{corr}} - \Delta\rho_{\mathrm{visc}} - \rho_{\mathrm{exact}})/\rho$ of refined solution from the analytical one, and bound of refined solution error (36) are presented. It can be seen that the main part of error is determined by viscosity and it may be computed and eliminated.

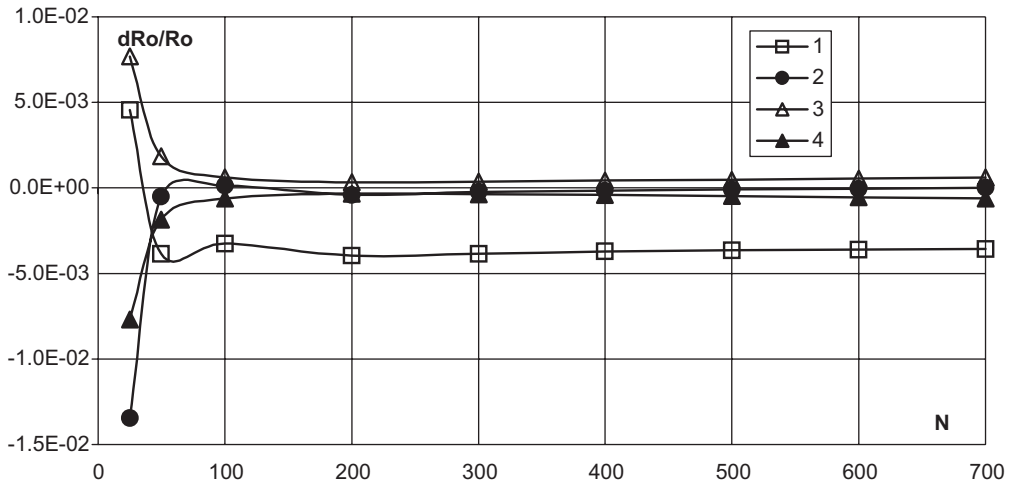

Figure 6. The error of calculation as a function of the reciprocal of mesh step (viscous flow, $Re = 1000$). 1—error due to viscous terms, 2—deviation of refined solution from analytical one, 3 and 4—bounds of error.

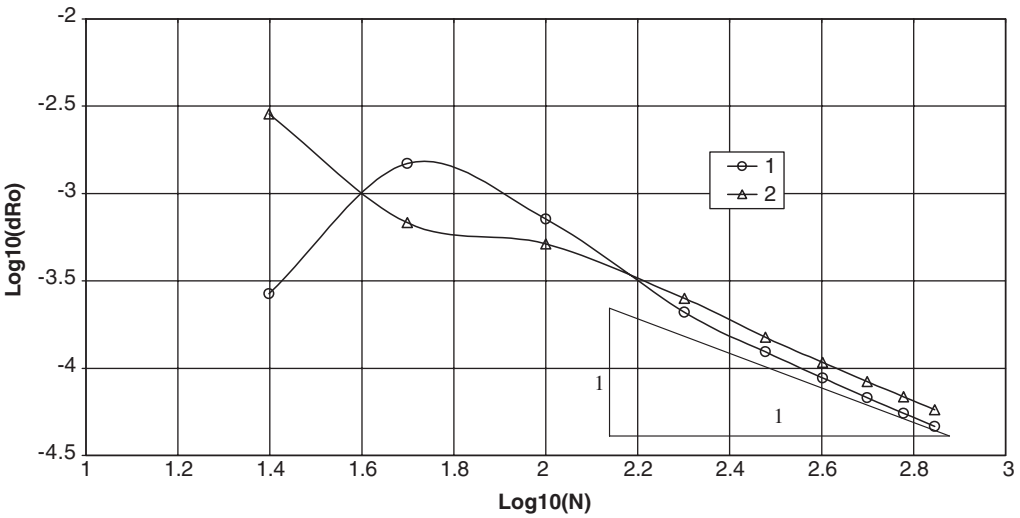

Figure 7. The error of calculation as a function of the reciprocal of mesh step (inviscid flow). 1—deviation of finite-difference solution from analytical one, 2—error correction according (37).

The refined result is close to analytical one and is located within the interval of error bound. Nevertheless, there is no convergence of error bound as expected from expression (36). Let us consider the related results for inviscid flow. Figure 7 presents the deviation of the finite-

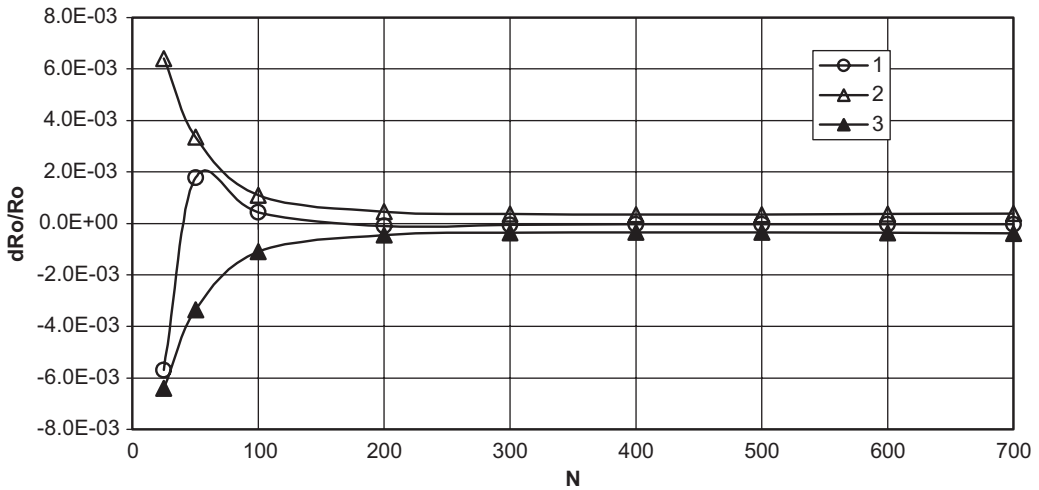

Figure 8. The error of calculation as a function of the reciprocal of mesh step (inviscid flow). 1—deviation of refined solution from analytical one, 2, 3—error bounds (38).

difference solution from the analytic one and correction of error in accordance with (35). The refinement of the solution using adjoint parameters according (35) enables the elimination of major part of the discretization error. The first order of computable error (35) may be detected if Figure 7 is analysed. Calculations demonstrated a good coincidence of the refined solution with analytical one and reliability of the error bound estimate (Figure 8). Nevertheless, the expectable second order of accuracy (36) does not manifest itself. When mesh is fine enough the error bound practically does not depend on the step size. This is caused by the growth of third derivatives of flow parameters as step size decreases. It may be due to the formation of weak discontinuities in the flowfield.

A comparison of Figures 6 and 8 demonstrates that the impact of viscosity effect using adjoint equations enables us to obtain result close to inviscid computation as far as accuracy is concerned. Thus, there exist feasibility for calculation of inviscid flow (Euler equations) and *a posteriori* error estimation on the basis of PNS. This extends the applicability of the considered method which is not directly applicable to the supersonic Euler equations due to the existence of discontinuous solutions.

Figure 9 presents the dependence of error of refined solution in the comparison with the initial error of solution (caused both by viscous terms and by approximation error) as a function of Re number. As the viscosity decreases, a certain increase of error bound estimate is visible due to growth of third derivatives of gasdynamical parameters. For small enough Re numbers the error of finite-difference calculation breaks the error bound that is caused by the significant distortion of flow pattern (compare Figure 2 ($Re = 1000$) and Figure 10 ($Re = 10$)).

In general, for a smooth flow the errors both for inviscid flow and for viscous flow (refined via adjoint parameters) are close.

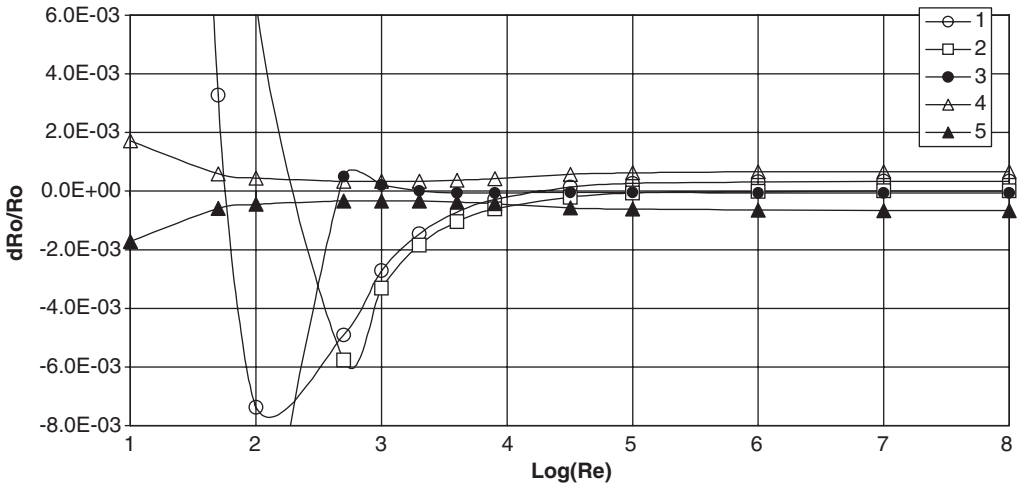

Figure 9. The error of calculation as a function of Reynolds number. 1—deviation of finite-difference solution from analytical one, 2—error due to viscous terms, 3—deviation of refined solution from analytical one, 4, 5—error bounds (38).

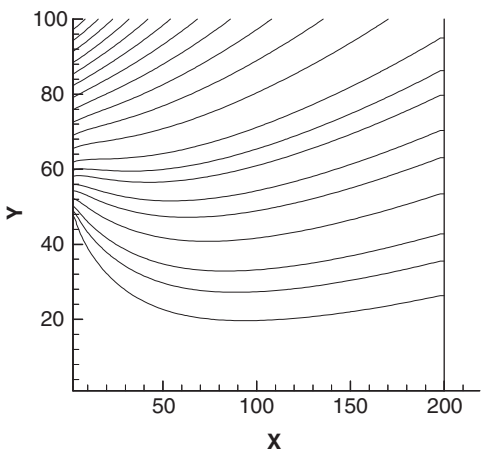

Figure 10. Isolines of density for small Re ($Re = 10$).

6.2. *Discontinuous flow field*

As another test, the error of the density past crossing shocks ($\alpha = \pm 22.23°$, $M = 4$, $Re = 1000$) is calculated. Figure 11 presents the density isolines within flowfield, Figure 12 illustrates isolines of the adjoint density, Figure 13 shows the density of error bound according (38), and Figure 14 presents isolines of the error caused by viscous terms.

This test is more complicated due to unbounded derivatives of gasdynamics parameters for inviscid flow. The presence of viscosity enables us to calculate flows with shocks, while at

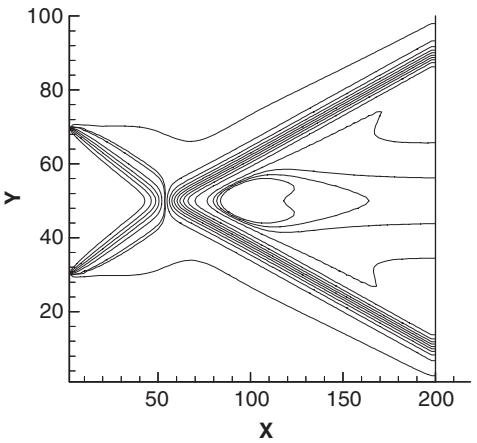

Figure 11. Isolines of density (crossing shocks).

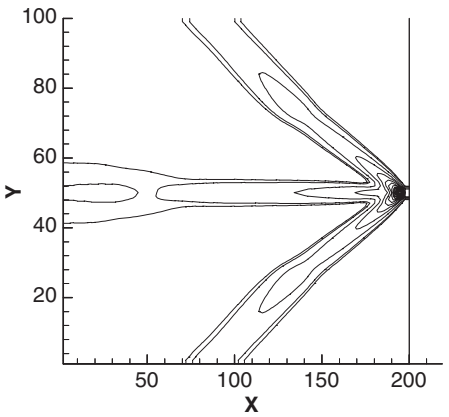

Figure 12. Isolines of adjoint density (concentration correlates with estimated point).

the same time it introduces an error proportional to $1/Re$. When viscosity decreases this error diminishes too, unfortunately the error related to unbounded derivatives increases simultaneously.

Figure 15 presents results for $Re = 1000$ as a function of the spatial step size. The viscous component of error is small enough, the deviation of the finite-difference solution from analytical one is small also and weakly depends on the step size, and this effect may be attributed to uncontrolled errors (the non-divergence of the scheme, possible).

Figure 16 presents results for inviscid flow as a function of the spatial step size. Both error and error bound have an order of convergence over grid size of $O(1)$.

Figure 17 shows the dependence of error on Reynolds number. As the viscosity decreases the error and error bound increase and approach the asymptote at the inviscid limit.

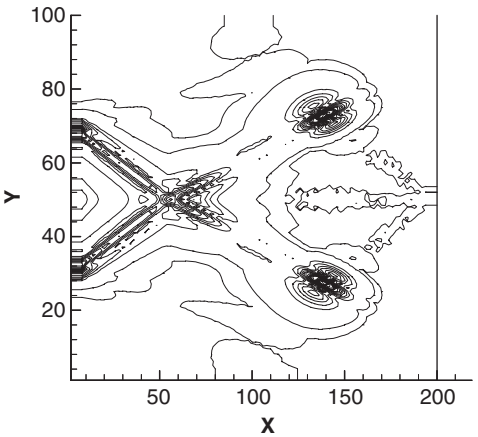

Figure 13. Isolines of error bound density (38).

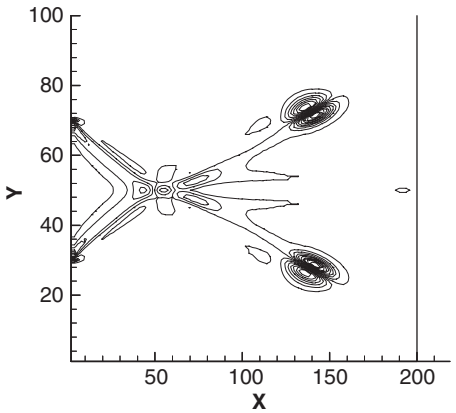

Figure 14. Isolines of error density caused by viscosity (23).

A natural way to eliminate errors connected with a non-divergent scheme is the choice of divergent one. The following systems of divergent Euler equations (two-dimensional) and related adjoint equations were used in numerical tests.

Divergent Euler equations:

$$\frac{\partial(\rho U^k)}{\partial X^k} = 0 \tag{40}$$

$$\frac{\partial(\rho U^k U^i + P\delta_{ik})}{\partial X^k} = 0 \tag{41}$$

$$\frac{\partial(\rho U^k h_0)}{\partial X^k} = 0 \tag{42}$$

Here $U^1 = U, U^2 = V$, $h(\rho, P) = \gamma e$ is the enthalpy, $h_0 = (U^2 + V^2)/2 + h$ is the total enthalpy.

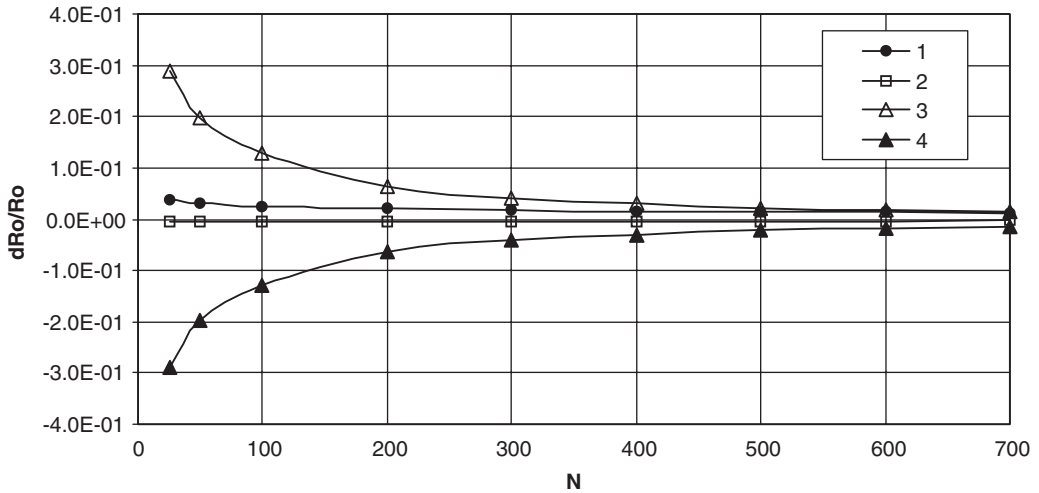

Figure 15. The error of calculation as a function of the reciprocal of mesh step (viscous flow). 1—deviation of refined solution from analytical one, 2—error density caused by viscosity (23), 3, 4—error bounds (38).

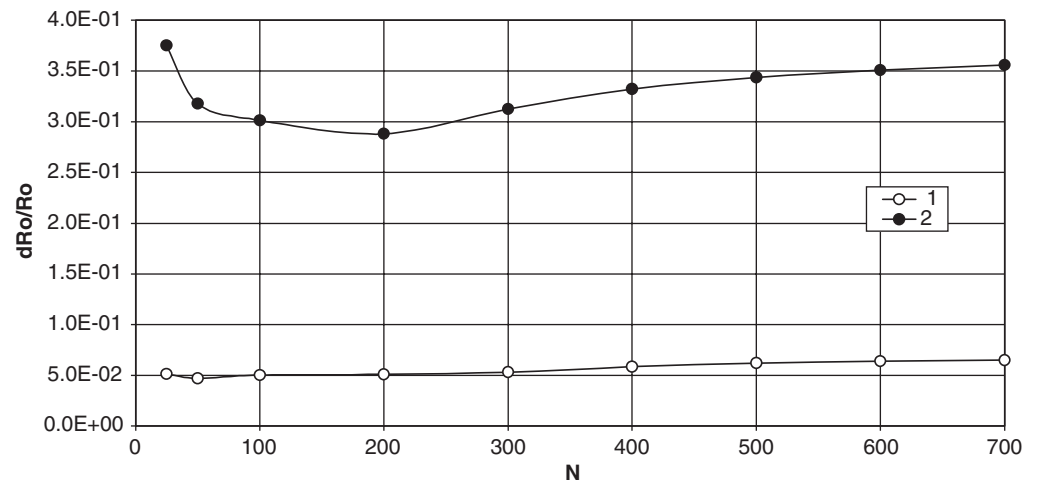

Figure 16. The error of calculation in dependence on the reciprocal of mesh step (inviscid flow). 1—deviation of refined solution from analytical one, 2—error bounds (38).

Adjoint equations:

$$U^k \frac{\partial \Psi_\rho}{\partial X^k} + U^k U^i \frac{\partial \Psi_i}{\partial X^k} + \frac{\gamma - 1}{\gamma} \frac{\partial \Psi_k}{\partial X^k}(h_0 - U_n U_n/2) + U^k h_0 \frac{\partial \Psi_h}{\partial X^k} = 0 \tag{43}$$

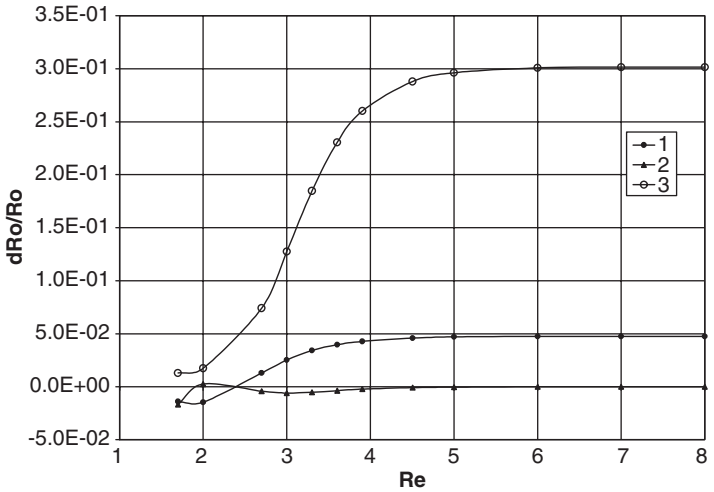

Figure 17. The error of calculation as a function of Reynolds number. 1—deviation of finite-difference solution from analytical one, 2—error caused by viscosity (23). 3—error bound (38).

$$U^i \frac{\partial \Psi_i}{\partial X^k} + U^i \frac{\partial \Psi_k}{\partial X^i} + \frac{\partial \Psi_\rho}{\partial X^k} + \frac{\gamma - 1}{\gamma} \frac{\partial \Psi_n}{\partial X^n} U_k + h_0 \frac{\partial \Psi_h}{\partial X^k} = 0 \tag{44}$$

$$U^k \frac{\partial \Psi_h}{\partial X^k} + \frac{\gamma - 1}{\gamma} \frac{\partial \Psi_k}{\partial X^k} = 0 \tag{45}$$

Several variants of first-order finite-difference schemes (two dimensional) were used, including 'donor cells' [47] and a scheme of Courant–Isaacson–Rees [48]. As expected, the deviation of finite-difference solution from analytic one for divergent scheme is significantly smaller compared with non-divergent one. Unfortunately, error estimates use derivatives that are unbounded in divergent case also (excluding one-dimensional flow). The results of test computations are analogous to results obtained using the non-divergent scheme. We may compare the grid convergence for non-divergent scheme (Figure 16) with results for divergent one (Figure 18, inviscid flow).

If we introduce viscosity, we can obtain convergent estimates of error for divergent scheme too (Figure 19).

The above tests are oriented towards comparison with analytical solutions that belong to inviscid flows. This creates some specifics. For example, the previous test flowfield is composed of regions of constant gasdynamical parameters separated by shocks. So, it is not the best problem from error estimates viewpoint using derivatives of gasdynamical parameters. Thus, it is expedient to consider a test problem more typical of viscous gas flows. Let us consider a viscous ($Re = 1000$) supersonic weakly underexpanded ($p_j/p_\infty = 2$) jet in supersonic flow. Figure 20 presents isolines of the density in flowfield, Figure 21 presents isolines of the adjoint density, and Figure 22 presents the spatial density of error bound estimate (38). Unfortunately, corresponding analytical solutions for this problem are unknown. Hence, the solution on the finest mesh was regarded as an 'exact' one. Figure 23 presents the error

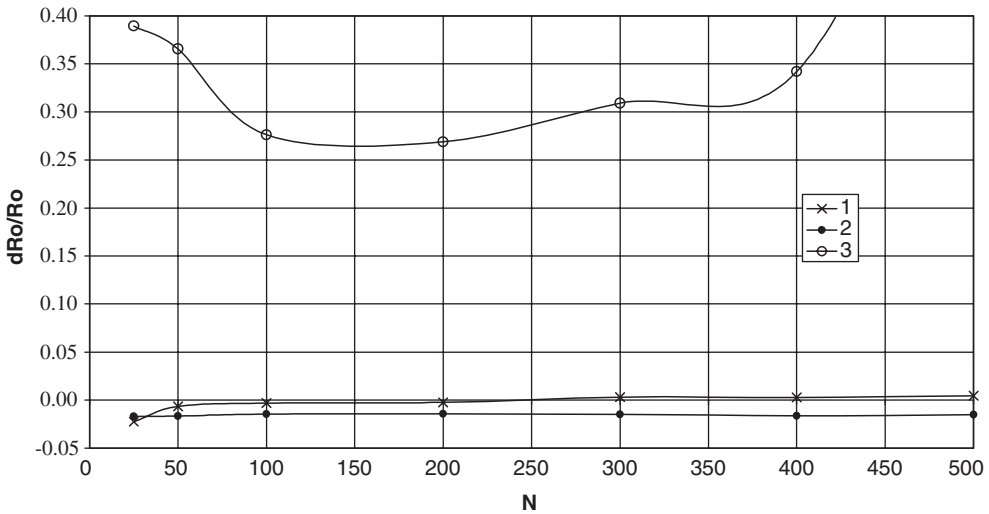

Figure 18. The error of calculation as a function of the reciprocal of mesh step (inviscid flow, divergent scheme). 1—deviation of finite-difference solution from analytical one, 2—correction (37), 3—bound of error.

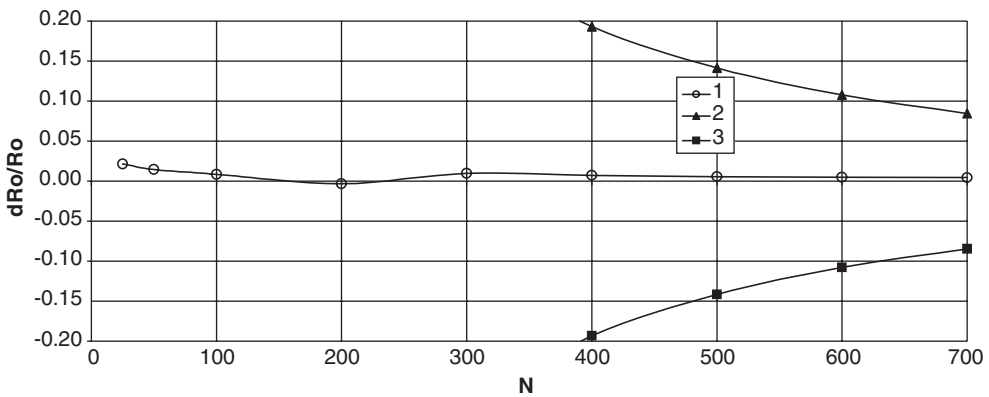

Figure 19. The error of calculation as a function of the reciprocal of mesh step (viscous flow, divergent scheme). 1—deviation of refined solution from analytical one, 2, 3–error bounds (38).

bound and the deviation of the solution from 'exact' one in dependence on the grid step. The convergence order for error bound is close to one (slightly below and decreases as the mesh is refined). This result may be an indirect evidence of presence of discontinuities in derivatives of gasdynamical parameters.

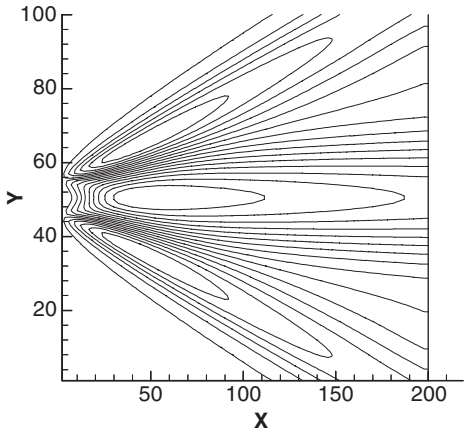

Figure 20. Isolines of density.

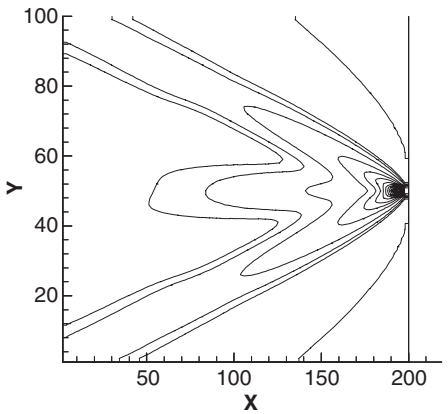

Figure 21. Isolines of adjoint density.

7. THE EVALUATION OF COMPUTABLE ERROR USING RESIDUAL

The residual based approach closely related to [19] is used herein for an estimation of computable error without explicit use of differential approximation. The main difference between this approach and that of [19] is in the residual calculation. We do not use an interpolation of flow parameters from grid points to total domain. Instead, we use a higher-order scheme on the same numerical solution. Let us consider this approach at a heuristic level. Assume we have a flowfield computed via certain finite-difference method. We try to estimate the error of this calculation. Let us use the equation $(\partial\tilde{\rho}/\partial t)+(\partial\tilde{\rho}/\partial x)=0$ as an example. Let the

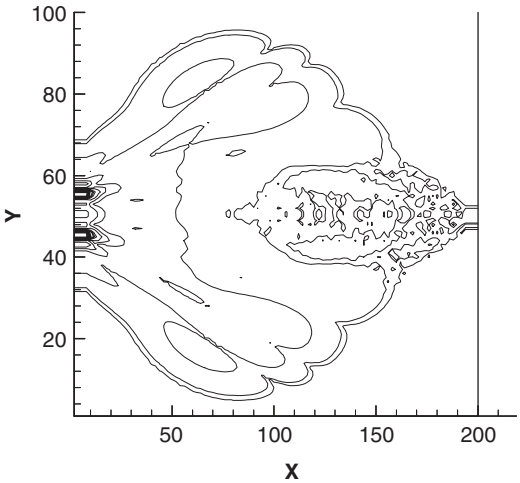

Figure 22. The density of error bound (38).

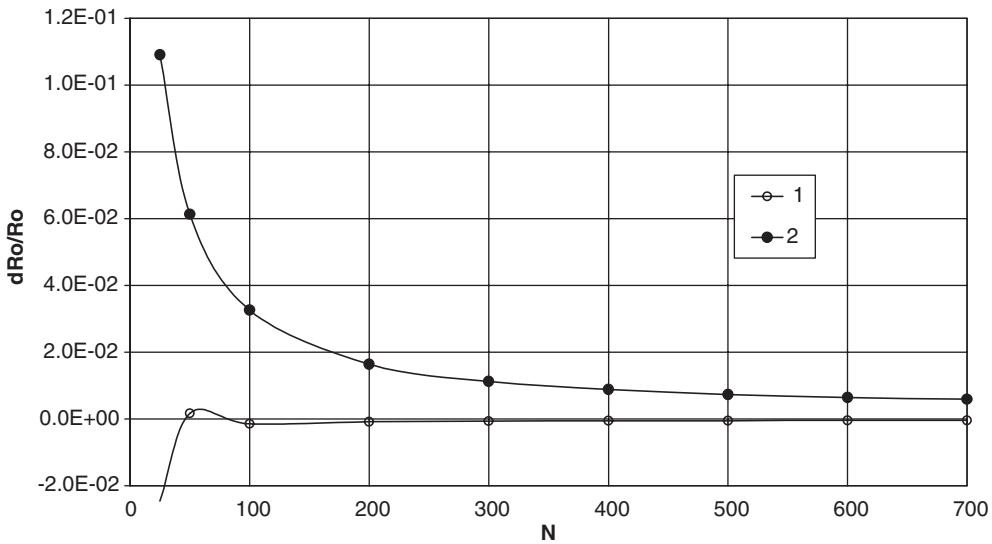

Figure 23. The error of calculation as a function of the reciprocal of mesh step. 1—deviation of refined solution from 'exact' one, 2—bound of error.

flowfield be calculated via first-order finite-difference approximation

$$\frac{\rho_k^{n+1} - \rho_k^n}{\tau} + \frac{\rho_{k+1}^n - \rho_k^n}{h_k} = 0 \tag{46}$$

The differential approximation of (44) may be written as $(\partial\rho/\partial t) + (\partial\rho/\partial x) + \delta\rho = 0$. Let us write it in more detail using a Taylor series with the remainder in a Lagrange form,

(parameters $\alpha_k^n \in (0,1), \beta_k^n \in (0,1)$ are unknown).

$$\frac{\partial \rho}{\partial t} + \frac{\partial \rho}{\partial x} + \frac{1}{2}\left(\tau \frac{\partial^2 \rho(t_n, x_k)}{\partial t^2} + h_k \frac{\partial^2 \rho(t_n, x_k)}{\partial x^2}\right) + \frac{\tau^2}{6}\frac{\partial^3 \rho(t_n + \beta_k^n \tau, x_k)}{\partial t^3}$$

$$+ \frac{h_k^2}{6}\frac{\partial^3 \rho(t_n, x_k + \alpha_k^n h_k)}{\partial x^3} = 0 \tag{47}$$

Let us replace (46) by the stencil of next (second) order of accuracy and calculate residual η_k^n, arising from applying the high-order scheme to the flowfield calculated using the low-order scheme.

$$\frac{\rho_k^{n+1} - \rho_k^{n-1}}{2\tau} + \frac{\rho_{k+1}^n - \rho_{k-1}^n}{2h_k} = \eta_k^n \tag{48}$$

Expression (48) may be expanded in the Taylor series as

$$\eta_k^n = \frac{\rho_k^{n+1} - \rho_k^{n-1}}{2\tau} + \frac{\rho_{k+1}^n - \rho_{k-1}^n}{2h_k}$$

$$= \frac{\partial \rho}{\partial t} + \frac{\tau^2}{6}\frac{\partial^3 \rho(t_n + \gamma_k^n \tau, x_k)}{\partial t^3} + \frac{\partial \rho}{\partial x} + \frac{h_k^2}{6}\frac{\partial^3 \rho(t_n, x_k + \chi_k^n h_k)}{\partial x^3} \tag{49}$$

The function ρ_k^n is obtained from solution of (46) and so complies with condition (47). Let us substitute (47) in (49), then the residual assumes the form

$$\eta_k^n = \frac{\tau^2}{6}\frac{\partial^3 \rho(t_n + \gamma_k^n \tau, x_k)}{\partial t^3} + \frac{h_k^2}{6}\frac{\partial^3 \rho(t_n, x_k + \chi_k^n h_k)}{\partial x^3}$$

$$-\frac{1}{2}\left(\tau \frac{\partial^2 \rho(t_n, x_k)}{\partial t^2} + h_k \frac{\partial^2 \rho(t_n, x_k)}{\partial x^2}\right) - \frac{\tau^2}{6}\frac{\partial^3 \rho(t_n + \beta_k^n \tau, x_k)}{\partial t^3}$$

$$-\frac{h_k^2}{6}\frac{\partial^3 \rho(t_n, x_k + \alpha_k^n h_k)}{\partial x^3} \tag{50}$$

Correspondingly, the lower-order term of truncation error (47) has a form

$$\frac{1}{2}\left(\tau \frac{\partial^2 \rho(t_n, x_k)}{\partial t^2} + h_k \frac{\partial^2 \rho(t_n, x_k)}{\partial x^2}\right) = -\eta_k^n + \frac{\tau^2}{6}\frac{\partial^3 \rho(t_n + \gamma_k^n \tau, x_k)}{\partial t^3} - \frac{\tau^2}{6}\frac{\partial^3 \rho(t_n + \beta_k^n \tau, x_k)}{\partial t^3}$$

$$+ \frac{h_k^2}{6}\frac{\partial^3 \rho(t_n, x_k + \chi_k^n h_k)}{\partial x^3}$$

$$-\frac{h_k^2}{6}\frac{\partial^3 \rho(t_n, x_k + \alpha_k^n h_k)}{\partial x^3} \approx \eta_k^n \tag{51}$$

Thus, the lower term of differential approximation (47) may be estimated via a residual obtained from using high-order stencil on the solution calculated using main finite-difference

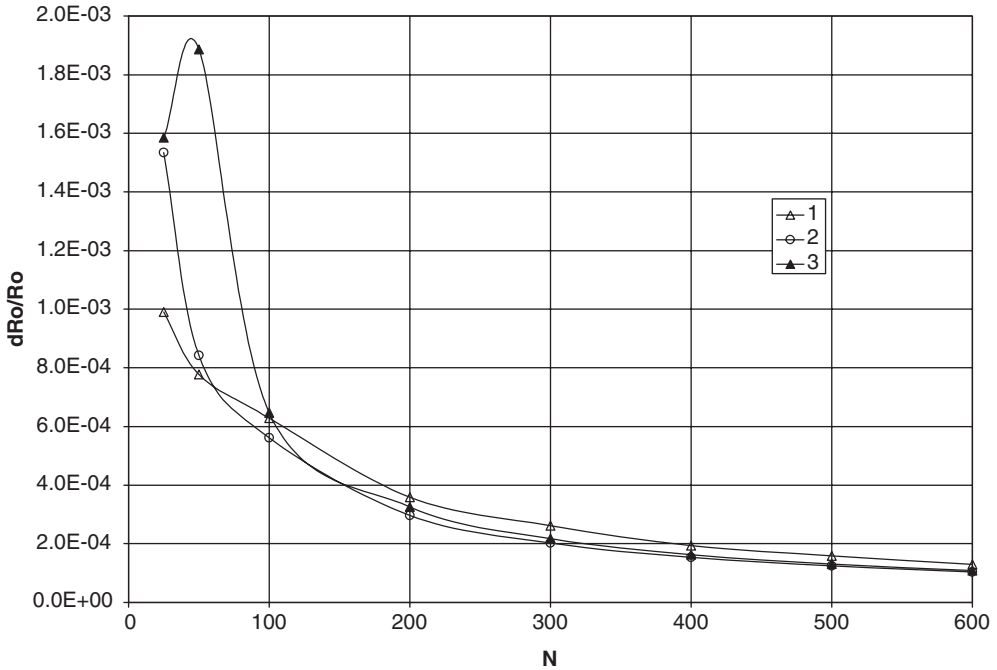

Figure 24. The comparison of different error evaluation as a function of the reciprocal of mesh step. 1—DA based error, 2—residual based error (52), 3—difference of the analytical and numerical values.

scheme. As a result we obtain the field of residuals that locally disturb the exact solution. According to (3) the variation of estimated value has a form $\Delta\varepsilon(\delta\rho) = \int_\Omega \delta\rho\psi \, \mathrm{d}t \, \mathrm{d}x$. Taking into account (51) we obtain

$$\Delta\varepsilon(\delta\rho) = \int_\Omega \delta\rho\psi \, \mathrm{d}t \, \mathrm{d}x \approx -\int_\Omega \eta\psi \, \mathrm{d}t \, \mathrm{d}x \tag{52}$$

In contrast to (3), expression (52) may be easily calculated without knowledge of differential approximation. On other hand, the differential approximation approach provides a more accurate account of higher terms and estimation of refined solution bounds. Let us compare these approaches using first-order upwind scheme and divergent form of Euler equations (38)–(43). For estimation of residual we use second-order approximation (48).

The deviation of calculation from analytical, the error estimation using DA based (35) and residual based methods are presented in Figure 24 for Prandtl–Mayer flow. The close correlation of estimates (35) and (52) for continuous flow is visible. If we recast Figure 24 on a logarithm scale, all these functions may be described by a first-order curve $O(h)$.

In contrast to (3) expression (52) may be extended to discontinuous flows if divergent finite difference schemes are used.

For discontinuous flow both derivatives in (48) are unbound, nevertheless these singularities are mutually compensated due to conservation law and the residual η_k^n is bounded. This residual

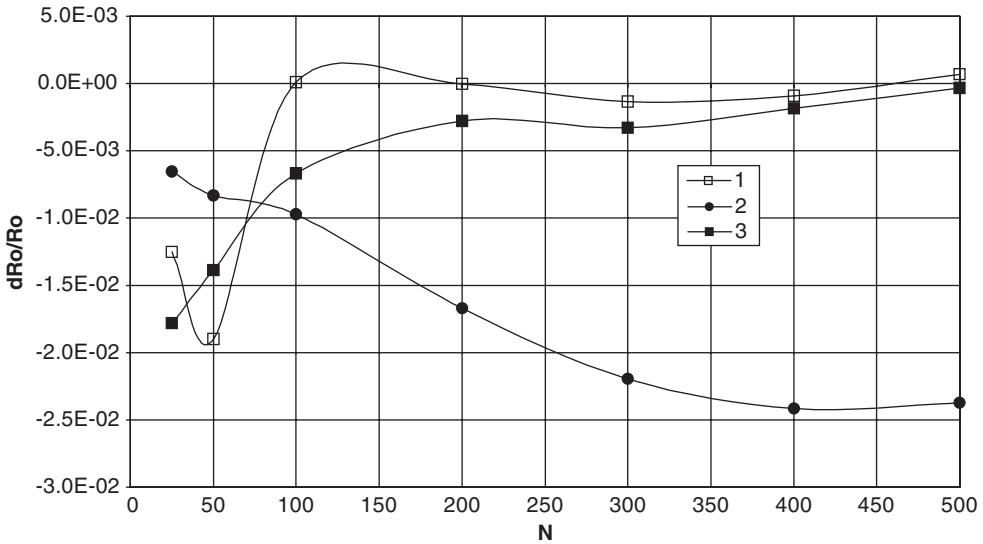

Figure 25. The errors as functions of the reciprocal of mesh step. 1—difference of the analytical and numerical values, 2—DA based error, 3—residual based error (52).

may be calculated using only a bounded combination of derivatives of flow parameters and applied for error estimation. A corresponding example is presented in Figure 25 for crossing shocks. It presents the error estimation using a residual based method (52), DA based (35) one, and the deviation of the calculation from the analytical value. Figure 25 demonstrates the residual approach (52) to provide a much more accurate estimation of error if compared with the differential approximation (35), which explicitly diverges. Unfortunately, the residual based approach does not provide an error bound.

8. DISCUSSION

The difficulties connected with using adjoint approach are of the same nature as those arising while using Richardson extrapolation. They are caused by the presence of discontinuities that determine the order of accuracy observable in numerical tests. Let us consider this problem at an heuristic level. For this purpose let us write (5) in more detail. Let m be the number of bounded derivatives (derivatives of the order m and higher may have a finite number of jump discontinuities), p is the order of the approximated derivative, j is the formal order of accuracy of a finite-difference scheme. Let us approximate derivatives by the finite differences $\mathrm{D}\rho(t,x)/\mathrm{D}x$. The limit

$$\lim_{h\to 0}\sum_{\Omega}\left(h^{j}\frac{\mathrm{D}^{p+j}\rho(t,x)}{\mathrm{D}x^{p+j}}\right)h\Psi\tau$$

corresponds to the first term (5). Consider its asymptotic form. The derivative of order $m+1$ has an asymptotic $(\rho_+^{(m)} - \rho_-^{(m)})/h \sim \Delta/h$ for the jump discontinuity, while the derivative of order $m+2$ has the asymptotic $(\Delta/h - 0/h)/h \sim \Delta/h^2$, correspondingly the derivative of the order $p+j$ has the asymptotic Δ/h^{p+j-m}. Thus

$$\lim_{h\to 0}\left(h^j \frac{\mathrm{D}^{p+j}\rho(t,x)}{\mathrm{D}x^{p+j}}\right) \sim \lim_{h\to 0}\left(h^j \frac{\Delta}{h^{p+j-m}}\right)$$

There is a limited number of nodes that participate in the summation in the vicinity of discontinuity, so the multiplier h (appearing during summation) should be taken into account, yielding

$$\sum_{k=1,n=n_r-n_s}^{k=Nx,n=n_r+n_s}\left(h^j \frac{\mathrm{D}^{p+j}\rho(t,x)}{\mathrm{D}x^{p+j}}\right) h\Psi\tau \sim h^{m-p+1}$$

Thus, the terms of jth formal order of accuracy contain a component of jth order (appearing due to integration over the smooth part of the solution) and a component having the order $i=m-p+1$ (engendered by the jump discontinuity of the mth order derivative). So, the order of convergence depends on the solution and may asymptotically tend to a minimal order $i=m-p+1$ as the grid size decreases. In Reference [38] the influence of discontinuities on the error is considered for example that of the spatial derivative of temperature.

The calculation of approximation errors by considered method requires the existence of bounded derivatives of relatively high order. They do not exist always, so, for supersonic Euler equations, these estimates may be calculated only for smooth solutions. If discontinuities are expected for the studied flow, the use of viscosity enables us to conduct these estimates. The viscosity engenders its own component of error, which may also be eliminated using adjoint equations. This approach permits to obtain error estimates for inviscid supersonic flows using this method.

Naturally, we can estimate not only the error of density written as a functional (15), but the error of other functionals. The differences are only in the form of the source terms in adjoint equations (16)–(19).

For justification of error estimates we should verify that the unaccounted error component induced by approximation error of adjoint equations is small enough. For calculation of this component we can solve second-order adjoint equations [39]. Such a suitable example is presented in Reference [38] for heat conduction equation.

For error estimates we use numerical results that may be significantly less smooth then the computed physical field. Thus, for certain finite-difference schemes (non-monotonic) the error bounds may be too large. The applicability of method considered above is restricted to numerical schemes which do not exhibit non-physical oscillations.

9. CONCLUSION

The computable pointwise error of viscous flow parameter caused by a finite-difference approximation may be evaluated using differential approximation terms and adjoint equations. The asymptotic bound of refined solution error may be determined simultaneously.

Numerical tests carried out demonstrated the efficiency of this method for parabolized Navier–Stokes. The influence of viscous terms may be calculated similarly and that provides also for feasibility of estimating errors of the Euler equations.

The computer time required for point-wise refining of a single parameter at a single point and error bound calculation is equal to the time required for flowfield calculation on the same grid.

NOMENCLATURE

C_v	specific volume heat capacity
e	specific energy, $C_v T$
f	flow parameters (ρ, U, V, e)
h	enthalpy
h_0	total enthalpy
h_x, h_y	spatial steps along X and Y
M	Mach number
N_t	number of time steps
N_x	number of spatial nodes along X
N	number of spatial nodes along Y
L	Lagrangian
P	pressure
P	Prandtl number ($Pr = \mu C_v/\lambda$)
R	gas constant
Re	Reynolds number ($Re = \rho_\infty U_\infty Y_{\max}/\mu_\infty$)
T	temperature
U	velocity component along X
V	velocity component along Y
X, Y	co-ordinates

Greek letters

α, β, γ	coefficients in Taylor–Lagrange series
δ	Dirac's delta function
$\Delta\rho_x^{\text{corr}}$	correctable error, connected with the expansion along X
$\Delta\rho^{\text{corr}}$	correctable error
$\Delta\rho_x^{\text{sup}}$	component of bound of inherent error, connected with the expansion in co-ordinate X
$\Delta\rho^{\text{sup}}$	component of bound of inherent error
γ	specific heat ratio
ε	functional
μ	viscosity
λ	thermal conductivity
ρ	density
τ	temporal step
$\Psi_\rho, \Psi_U, \Psi_V, \Psi_e$	adjoint variables
Ω	domain of calculation

Subscripts

∞	entrance boundary parameters
an	analytical solution
corr	corrected error
est	estimated point
exact	exact solution
k	number of spatial mesh node along Y
n	number of step along X
sup	bound of inherent error
x	component of truncation error connected with Taylor expansion in co-ordinate X
t	component of truncation error connected with Taylor expansion in time

ACKNOWLEDGEMENTS

The second author would like to acknowledge support of NSF Grant ATM-0201808 managed by Dr Lydia Gates.

REFERENCES

1. Marchuk GI, Shaidurov VV. *Difference Methods and their Extrapolations.* Springer: New York, 1983.
2. Roache PJ. Quantification of uncertainty in computational fluid dynamics. *Annual Review of Fluid Mechanics* 1997; **29**:123–160.
3. Roy CJ. Grid convergence error analysis for mixed-order numerical schemes. *AIAA Journal* 2003; **41**(4): 595–604.
4. Carpenter MH, Casper JH. Accuracy of shock capturing in two spatial dimensions. *AIAA Journal* 1999; **37**(9):1072–1079.
5. Efraimsson G, Kreiss G. A remark on numerical errors downstream of slightly viscous shocks. *SIAM Journal on Numerical Analysis* 1999; **36**(3):853–863.
6. Engquist B, Sjogreen B. The convergence rate of finite difference schemes in the presence of shocks. *SIAM Journal on Numerical Analysis* 1998; **35**:2464–2485.
7. Roy CJ, McWherter-Payne MA, Oberkampf WL. Verification and validation for laminar hypersonic flowfields. *AIAA Journal* 2003; **41**(10):1944–1954.
8. Yamaleev NK, Carpenter MH. On accuracy of adaptive grid methods for captured shocks. *NASA/TM-2002-211415*; 1–37.
9. Ainsworth M, Oden JT. *A Posteriori Error Estimation in Finite Element Analysis*. Wiley-Interscience: New York, 2000.
10. Oden JT, Prudhomme S. Goal-oriented error estimation and adaptivity for the finite element method. *Computers and Mathematics with Applications* 2001; **41**:735–756.
11. Oden JT, Prudhomme S. Estimation of modeling error in computational mechanics. *Journal of Computational Physics* 2002; **182**:496–515.
12. Oden JT, Prudhomme S. On goal-oriented error estimation for elliptic problems: application to the control of pointwise errors. *Computer Methods in Applied Mechanics and Engineering* 1999; **176**:313–331.
13. Johnson C. On computability and error control in CFD. *International Journal for Numerical Methods in Fluids* 1995; **20**:777–788.
14. Hoffman J, Johnson C. Computability and adaptivity in CFD. In *Encyclopedia of Computational Mechanics*, *vol. 3: Fluids*, Stein E, de Borst R, Hughes TJR (eds). Wiley: Chichester, 2004.
15. Hartmann R, Houston P. Goal-oriented *a posteriori* error estimation for compressible fluid flows. In *Numerical Mathematics and Advanced Applications*, Brezzi F, Buffa A, Corsaro S, Murli A (eds). Springer: Berlin, 2003; 775–784.
16. Venditti D, Darmofal D. Adjoint error estimation and grid adaptation for functional outputs: application to quasi-one-dimensional flow. *Journal of Computational Physics* 2000; **164**:204–227.

17. Venditti D, Darmofal D. Grid adaptation for functional outputs: application to two-dimensional inviscid flow. *Journal of Computational Physics* 2002; **176**:40–69.
18. Darmofal D, Venditti D. Anisotropic grid adaptation for functional outputs: application to two-dimensional viscous flows. *Journal of Computational Physics* 2003; **187**:22–46.
19. Giles MB. On adjoint equations for error analysis and optimal grid adaptation in CFD. In *Computing the Future II: Advances and Prospects in Computational Aerodynamics*, Hafez M, Caughey DA (eds). Wiley: New York, 1998; 155–170.
20. Pierce NA, Giles MB. Adjoint recovery of superconvergent functionals from PDE approximations. *SIAM Review* 2000; **42**:247–264.
21. Giles M, Pierce NA. Improved lift and drag estimates using adjoint euler equations. *Technical Report 99-3293*, AIAA, Reno, NV, 1999; 1–12.
22. Park MA. Three-dimensional turbulent RANS adjoint-based error correction. *AIAA Paper 2003-3849*; 1–14.
23. Park MA. Adjoint-based, three-dimensional error prediction and grid adaptation. *AIAA Paper 2002-3286*, 2002; 1–11.
24. Giles MB, Suli E. Adjoint methods for PDEs: *a posteriori* error analysis and postprocessing by duality. *Acta Numerica* 2002; **11**:145–206.
25. Giles MB, Pierce NA, Suli E. Progress in adjoint error correction for integral functionals. *Computing and Visualization in Science* 2004; **6**:113–121.
26. Pierce NA, Giles MB. Adjoint and defect error bounding and correction for functional estimates. *Journal of Computational Physics* 2004; **200**:769–794.
27. Pierce NA, Giles MB. Adjoint and defect error bounding and correction for functional estimates. *AIAA Paper* 2003; 3846.
28. Bangerth W, Rannacher R. Finite element approximation of the acoustic wave equation: error control and mesh refinement. *East–West Journal of Numerical Mathematics* 1996; **7**(4):263–282.
29. Becker R, Rannacher R. An optimal control approach to *a posteriori* error estimation in finite element methods. In *Acta Numerica*, Iserles A (ed.). Cambridge University Press: Cambridge, 2001; 1–102.
30. Heuveline V, Rannacher R. Duality-based adaptivity in the hp-finite element method. *Journal of Numerical Mathematics* 2003; **11**(2):1–18.
31. Houston P, Rannacher R, Suli E. *A posteriori* error analysis for stabilized finite element approximations of transport problems. *Computer Methods in Applied Mechanics and Engineering* 2000; **190**(11–12):1483–1508.
32. Monk P, Suli E. The adaptive computation of far field patterns by *a posteriori* error estimates of linear functionals. *SIAM Journal on Numerical Analysis* 1998; **36**(1):251–274.
33. Suli E, Houston P. Adjoint error correction for integral outputs. *Adaptive Finite Element Approximation of Hyperbolic Problems*. Springer: Berlin, 2002.
34. Suli E, Houston P. Finite element methods for hyperbolic problems: *a posteriori* error analysis and adaptivity. In *The State of the Art in Numerical Analysis*, Duff I, Watson GA (eds). Oxford University Press: Oxford, 1997; 441–471.
35. Suli E. *A posteriori* error analysis and adaptivity for finite element approximations of hyperbolic problems. In *An Introduction to Recent Developments in Theory and Numerics for Conservation Laws*, Kruner D, Ohlberger M, Rohde C (eds), Lecture Notes in Computational Science and Engineering, vol. 5. Springer: Berlin, 1998; 123–194.
36. Shokin YuI. *Method of Differential Approximation*. Springer: Berlin, 1983.
37. Alekseev AK. Control of an error of a finite-difference solution of the heat-conduction equation by the conjugate equation. *Journal of Engineering Physics and Thermophysics* 2004; **77**(1):177–184.
38. Alekseev AK, Navon IM. On *a-posteriori* pointwise error estimation using adjoint temperature and Lagrange remainder. *Computer Methods in Applied Mechanics and Engineering*, 2004, in press.
39. Wang Z, Navon IM, Le Dimet FX, Zou X. The second order adjoint analysis: theory and applications. *Meteorology and Atmospheric Physics* 1992; **50**:3–20.
40. Alekseev A, Navon M. On estimation of temperature uncertainty using the second order adjoint problem. *International Journal of Computational Fluid Dynamics* 2002; **16**(2):113–117.
41. Marchuk GI. *Adjoint Equations and Analysis of Complex Systems*. Kluwer Academic Publishers: Dordrecht, Hardbound, 1995.
42. Alekseev AK. 2D inverse convection dominated problem for estimation of inflow parameters from outflow measurements. *Inverse Problems in Engineering* 2000; **8**:413–434.
43. Alekseev AK, Navon IM. Calculation of uncertainty propagation using adjoint equations. *International Journal of Computational Fluid Dynamics* 2003; **17**(4):283–288.
44. Lions JL. Pointwise control of distributed systems. In *Control and Estimation in Distributed Parameter Systems*, Banks HT (ed.), Frontiers in Applied Mathematics, vol. 11. SIAM: Philadelphia, PA, 1992; 1–39.
45. Tornberg AK, Engquist B. Regularization techniques for numerical approximation of PDEs with singularities. *Journal of Scientific Computing* 2003; **19**:527–552.

46. Walden J. On the approximation of singular source terms in differential equations. *Numerical Methods for Partial Differential Equations* 1999; **15**:503–520.
47. Roache P. *Computational Fluid Dynamics*. Hermosa: Albuquerque, New Mexico, 1976.
48. Kulikovskii AG, Pogorelov NV, Semenov AYu. *Mathematical Aspects of Numerical Solution of Hyperbolic Systems*. Monographs and Surveys in Pure and Applied Mathematics, vol. 188. Chapman & Hall/CRC: Boca Raton, FL, 2001.

